Molecular Microbiology (2010) 76(4), 905–917 ■
doi:10.1111/j.1365-2958.2010.07143.x
First published online 8 April 2010

Pneumococcal CbpD is a murein hydrolase that requires a dual cell envelope binding specificity to kill target cells during fratricide

Vegard Eldholm,[1] Ola Johnsborg,[1] Daniel Straume,[1] Hilde Solheim Ohnstad,[1] Kari Helene Berg,[1] Juan A. Hermoso[2] and Leiv Sigve Håvarstein[1]*

[1]*Department of Chemistry, Biotechnology and Food Science, Norwegian University of Life Sciences, N-1432, Ås, Norway.*

[2]*Grupo de Cristalografía Macromolecular y Biología Estructural, Instituto Química-Física Rocasolano, CSIC, Serrano 119, 28006-Madrid, Spain.*

Summary

Pneumococci that are competent for natural genetic transformation express a number of proteins involved in binding, uptake, translocation and recombination of DNA. In addition, they attack and lyse non-competent sister cells present in the same environment. This phenomenon has been termed fratricide. The key effector of pneumococcal fratricide is CbpD, a secreted protein encompassing an N-terminal CHAP domain, two SH3b domains and a C-terminal choline-binding domain (CBD). CbpD is believed to degrade the cell wall of target cells, but experimental evidence supporting this hypothesis has been lacking. Here, we show that CbpD indeed has muralytic activity, and that this activity requires functional CBD and SH3b domains. To better understand the critical role played by the non-catalytic C-terminal region of CbpD, various translational fusions were constructed between the CBD and SH3b domains and green fluorescent protein (GFP). The results showed that the SH3b domains specifically recognize and bind peptidoglycan, while the CBD domain functions as a localization signal that directs CbpD to the septal region of the pneumococcal cell. Intriguingly, transmission electron microscopy analysis revealed that target cells attacked by CbpD ruptures at the septal region, in accordance with the binding specificity displayed by the CBD domain.

Accepted 16 March, 2010. *For correspondence. E-mail sigve.havarstein@umb.no; Tel. (+47) 64965883; Fax (+47) 64965901.

Introduction

Pneumococci that are competent for natural genetic transformation kill and lyse non-competent sister cells or members of related species that are present in the same environment (for reviews, see Claverys and Håvarstein, 2007; Johnsborg and Håvarstein, 2009). This phenomenon has been termed fratricide. Proteins that are involved in the fratricide mechanism are encoded by early and late competence genes, and are consequently an integral part of the competence regulon. When pneumococci grow under conditions that are permissive for competence development they secrete a peptide pheromone (CSP) that regulates competence development by a quorum-sensing-like mechanism (Håvarstein *et al.*, 1995). By analogy with other two-component signal transduction systems, binding of extracellular CSP to its membrane-bound histidine kinase receptor, ComD, presumably results in transfer of a phosphoryl group to the cognate response regulator ComE (Håvarstein *et al.*, 1996; Pestova *et al.*, 1996). ComE then activates transcription of the early competence genes (Ween *et al.*, 1999), including the genes encoding the immunity protein ComM and the alternative σ-factor ComX (Lee and Morrison, 1999; Håvarstein *et al.*, 2006). ComM, which is predicted to be a polytopic integral membrane protein, protects competent cells against committing suicide by an unknown mechanism. ComX is required for transcriptional activation of the late competence genes, several of which are involved in pneumococcal fratricide. These are the genes encoding the key fratricide effector CbpD, two bacteriocins (CibAB) and the amidase LytA (Guiral *et al.*, 2005; Kausmally *et al.*, 2005). LytA is synthesized by non-competent cells, but its rate of expression increases during competence (Mortier-Barrière *et al.*, 1998). The only important component of the fratricide mechanism that is not part of the competence regulon is the lysozyme LytC, whose expression depends on σ^{70} (Guiral *et al.*, 2005). CbpD causes some lysis of target cells on its own, but its effect is multiplied manyfold by its activation of LytA and LytC (Eldholm *et al.*, 2009). The combined action of CbpD, LytA and LytC enables *Streptococcus pneumoniae* to lyse both non-competent pneumococci and related

species such as *Streptococcus mitis* and *Streptococcus oralis* (Johnsborg *et al*., 2008). As lysis coincides with competence, DNA released from target cells is taken up by competent attacker cells, resulting in increased efficiency of gene transfer (Steinmoen *et al*., 2002; Johnsborg *et al*., 2008).

CbpD, LytA, LytC and CibAB all contribute to fratricide when mixed cultures of attacker and target cells are grown on blood agar plates (Guiral *et al*., 2005). In liquid culture, however, CbpD together with LytA and LytC are the major players (Eldholm *et al*., 2009). CbpD is a modular enzyme consisting of an N-terminal CHAP domain followed by two bacterial SH3 (SH3b) domains and a C-terminal choline-binding domain (CBD) comprising four repeat units. The enzymatic specificity of the CHAP domain has not been determined, but it displays significant homology with corresponding domains found in a number of phage lysins and bacterial murein hydrolases. Characterized members of the CHAP family have been found to act either as endopeptidases that cleave within murein stem peptides, or as amidases that cleave the *N*-acetylmuramyl-L-Ala bond (Bateman and Rawlings, 2003; Rigden *et al*., 2003; Layec *et al*., 2009). In eukaryotes, SH3 domains confer upon their resident proteins the ability to interact with specific proline-rich sequences in various protein binding partners (Wu *et al*., 1991). Bacterial SH3 domains (Whisstock and Lesk, 1999) are poorly characterized compared with their eukaryotic counterparts, but available evidence suggests that they recognize bacterial peptidoglycan (Baba and Schneewind, 1996; Lu *et al*., 2006). Proteins harbouring CBDs bind non-covalently to choline moieties decorating the wall- and lipoteichoic acids of *S. pneumoniae* and related streptococci. CBDs consist of a variable number of tandem repeat units, each of which is 20–21 amino acids in length. Choline binding sites are located at the interface of two consecutive repeat units, where three structurally conserved aromatic residues form a cavity in which the choline quaternary ammonium moiety is primarily stabilized by cation-π interactions with the aromatic side chains. CbpD and LytA harbours four and six repeat units at their C-terminal ends, respectively, while the CBD of LytC consists of eleven N-terminally located repeat units (García *et al*., 1999; Varea *et al*., 2000).

In the present article we have shown experimentally that CbpD is a murein hydrolase, and that its ability to cleave stem peptides in the pneumococcal cell wall enhances LytC-mediated murein hydrolysis. Cellular localization studies using various green fluorescent protein (GFP) fusions demonstrated that the SH3b domains of CbpD bind specifically to peptidoglycan, while the choline-binding domain directs CbpD to the division zone. Furthermore, dual binding of the CbpD to teichoic acid and peptidoglycan via its CBD and SH3b domains, respectively, was shown to be required for efficient lysis of target cells. Finally, we used transmission electron microscopy (TEM) to show that target cells rupture at the division zone when attacked by CbpD, in accordance with the fact that CbpD predominantly accumulates in the septal region.

Results

CbpD is a murein hydrolase

CbpD is synthesized by pneumococci when they enter the competent state, and is secreted to the extracellular milieu via the Sec apparatus. Our previous studies revealed that a minor fraction of the secreted CbpD proteins is released to the growth medium, while the major fraction associates with the surface of the competent producer cells. This fraction could be eluted by 2% choline, demonstrating that cell-surface attachment of CbpD occurs mainly by non-covalent binding to teichoic acid via the choline-binding domain of the protein (Eldholm *et al*., 2009). CbpD is an essential component of the fratricide mechanism, but is not able to cause substantial lysis of target cells by itself in mixed cultures. Instead, CbpD activates the autolysins LytA and LytC, which in the presence of CbpD efficiently degrade the cell wall of non-immune cells. How CbpD activates these autolysins are not known. However, due to the presence of a CHAP domain at the N-terminus of CbpD, it has been assumed that it functions as an amidase or peptidase that catalyses the hydrolysis of peptide bonds in the cell wall cross-bridges. To verify this hypothesis we performed a zymogram analysis of total protein extracts prepared from various *S. pneumoniae* mutants to assay for murein hydrolase activity of CbpD. Proteins in the extracts were separated by SDS-PAGE on a gel containing heat-killed cells from a *S. pneumoniae* Δ*lytA*, Δ*lytC* double mutant (RH16). The zymogram analysis established for the first time that CbpD is indeed a murein hydrolase (Fig. 1A). The zymograms also showed that CbpD is present only in extracts from competent cells, whereas active LytA and LytC are present in the extracts regardless of competence induction.

The finding that CbpD functions as a murein hydrolase that by the nature of its CHAP domain must cleave amide or peptide bonds in the stem peptides of pneumococcal peptidoglycan rises the question of whether this process is responsible for triggering the activity of the amidase LytA and the lysozyme LytC. It has been demonstrated previously that exchanging the catalytic cysteine in the CHAP domain of CbpD with an alanine, or alkylating it with iodoacetamide, abolishes the enzyme's ability to activate LytA and LytC (Håvarstein *et al*., 2006; Eldholm *et al*., 2009), a result that together with the fact that CbpD

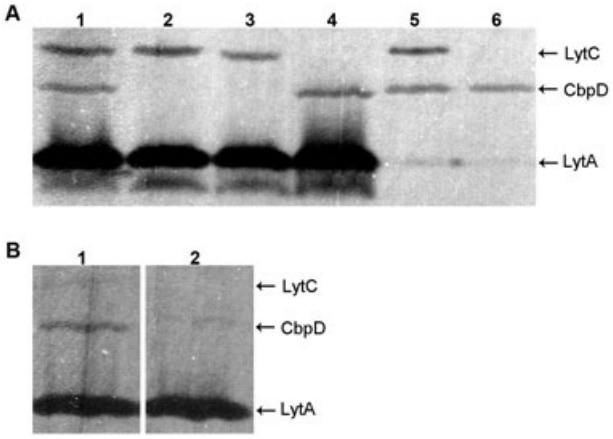

Fig. 1. Identification of pneumococcal murein hydrolases by zymography.
A. Zymogram analysis of total cell extracts prepared from various mutants of *S. pneumoniae*. Lytic activity was observed as bands of clear zones in the opaque gel. The lytic zones appear dark as the gels were photographed against a dark background. Competence-induced cells were harvested 15 min after addition of CSP (+). Uninduced cells were run in parallel without CSP (–). Lane 1: Wt + (strain RH1); lane 2: Wt – (strain RH1); lane 3: Δ*cbpD* + (strain RH17); lane 4: Δ*lytC* + (strain RH15); lane 5: Δ*lytA* + (strain RH14); lane 6: Δ*lytA*, Δ*lytC* + (strain RH16). Heat-inactivated cells of strain RH16 were incorporated in the SDS-PAGE gel. The zymograms were developed for 8 h.
B. Zymogram analysis of total cell extracts prepared from competence-induced RH1 cells harvested 15 min after addition of CSP. Heat-inactivated cells from strain RH14 (Δ*lytA*) were used in the zymogram depicted in lane 1, whereas cells from strain RH16 (Δ*lytA*, Δ*lytC*) were used in lane 2. The zymograms were developed for 1 h.

is a murein hydrolase proves that it is the amidase/endopeptidase function of CbpD that triggers the activity of the two autolysins. It follows from this that the combined action of CbpD and LytC should be more effective than CbpD alone in a zymogram assay like the one shown in Fig. 1A. To verify this, we compared the activity of CbpD in two different experimental set-ups. In one type of experiment, non-competent pneumococcal cells lacking both LytA and LytC were incorporated in the SDS-PAGE gel as a substrate for CbpD. In this case the clearing zone associated with CbpD resulted from the activity of this enzyme alone. In a parallel experiment the non-competent pneumococcal cells incorporated in the SDS-PAGE gel lacked only LytA. Consequently, the lysozyme LytC would be present in the cell wall of the cells attacked by CbpD, and should be activated by the action of this amidase/endopeptidase. The results of the zymogram analyses showed that the clearing zone caused by the combined action of CbpD and LytC appeared much faster and was more pronounced than the zone originating from the action of CbpD alone (Fig. 1B). It was not possible to perform a corresponding experiment with LytA proficient and deficient cells incorporated as substrate in the SDS-PAGE gels, because the presence of LytA caused complete lysis of the substrate making it impossible to detect the activity of CbpD and other murein hydrolases.

CbpD primarily targets the division zone

CbpD contains two SH3b domains and a CBD consisting of four repeat units. It is likely that both domain types are involved in attaching the protein to the cell envelope of target cells. CBDs specifically recognize and reversibly bind choline residues decorating teichoic and lipoteichoic acid in the cell wall of pneumococci (López *et al*., 2000; Hakenbeck *et al*., 2009). Bacterial SH3 domains are often part of proteins targeting the cell surface, suggesting that this type of domain recognizes the peptidoglycan, teichoic acid or some other part of the cell envelope. In the case of the lysostaphin homologue ALE-1, a murein hydrolase that specifically degrades *Staphylococcus aureus* cell walls, it has been reported that its C-terminal SH3b domain bind purified peptidoglycan in a manner that requires intact pentaglycine cross-bridges (Lu *et al*., 2006). To investigate whether CbpD targets a particular part of the pneumococcal cell envelope or binds evenly across the entire cell surface, we fused GFP to the C-terminal SH3b and choline-binding domains of CbpD. This was done by replacing the CHAP domain with GFP. The resulting fluorescent protein GFP–SH3b–SH3b–CBD was of similar size, and had the same number of domains as CbpD. In addition, an N-terminal His-tag was added to facilitate purification of the recombinant protein after overexpression in *Escherichia coli.* Our results show that the fusion protein mainly targets the division zone and poles of pneumococcal cells (Fig. 2A), but weak binding to the remaining part of the cell surface could be detected when longer exposure times were employed (data not shown).

The choline-binding module alone is sufficient to target CbpD to the division zone

The affinity of CbpD for the septal region could in principle be due to the SH3b domains, the choline-binding domain or both. To investigate these matters we expressed recombinant proteins engineered to contain a His-tagged GFP fused to different parts of CbpD. As cell wall teichoic acid (WTA) and lipoteichoic acid (LTA) are believed to be distributed evenly across the cell surface we considered it unlikely that the choline-binding domain is responsible for the observed binding pattern of CbpD (see Fig. 2A). We therefore initially focused on the SH3b domains. First, we deleted both SH3b domains and fused His-GFP directly to the choline-binding domain. Surprisingly, the resulting GFP–CBD product displayed the same binding pattern as the original GFP–SH3b–SH3b–CBD fusion protein (Fig. 2B). Even though each of the four domains of CbpD

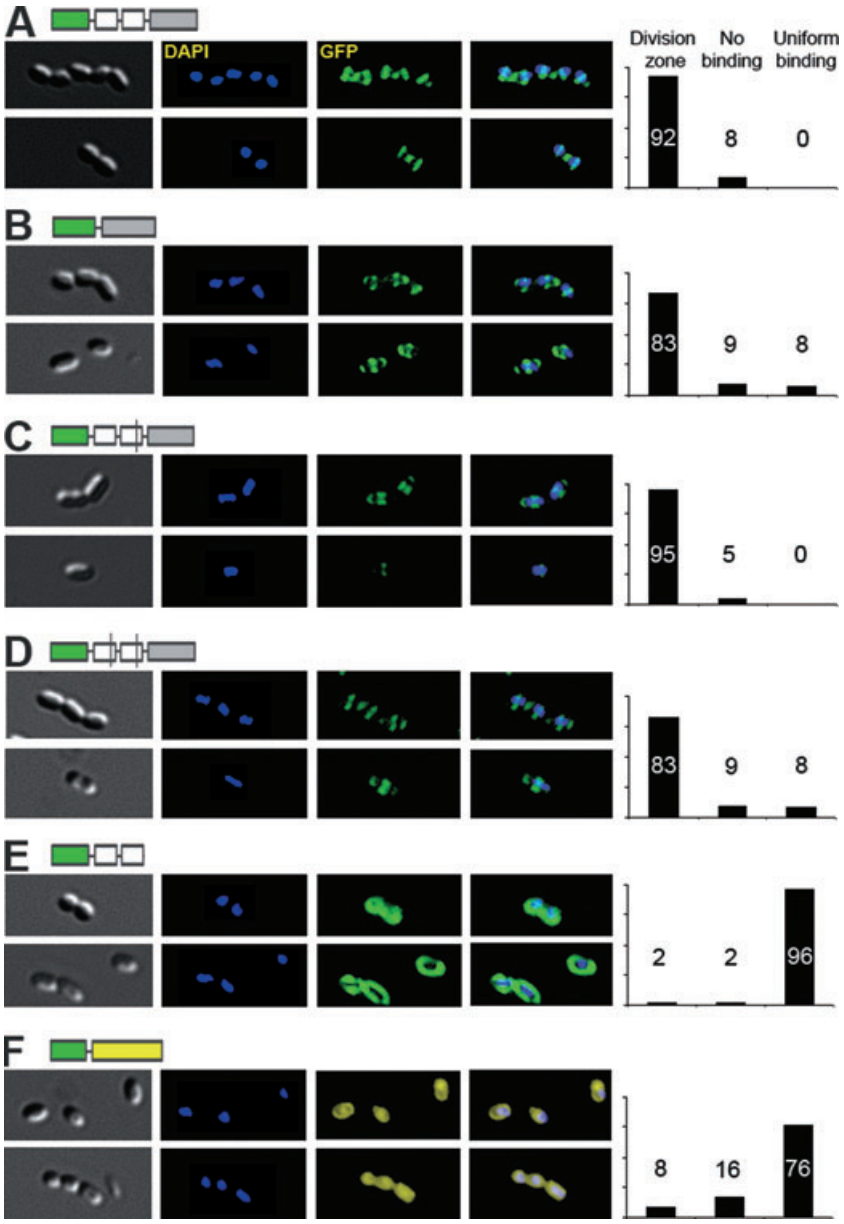

Fig. 2. Binding of various GFP fusion constructs to the surface of the *S. pneumoniae* RH14 strain. Green box represents GFP, open box represents a SH3b domain, grey box represents CBD from CbpD, yellow box represents CBD from CbpF. Vertical bars represent $W_{310}\rightarrow A$ and $W_{234}\rightarrow A$ mutations. Binding of the construct consisting of GFP fused to the CBD from CbpF is pseudocoloured yellow. Bars on the right-hand side show the distribution in per cent of the tree types of binding patterns observed with the different GFP fusion constructs.

is separated by a linker region, the possibility exists that deletion of the SH3b domains causes misfolding or affects the functionality of the downstream choline-binding domain. To inactivate the two SH3b domains without deleting them, highly conserved tryptophans at positions 234 and 310 were changed to alanines resulting in the constructs GFP–SH3b–SH3b$_{W310A}$–CBD and GFP–SH3b$_{W234A}$–SH3b$_{W310A}$–CBD (see Fig. 3B). Both of these mutated proteins targeted the septal and polar regions of the pneumococcal cell envelope, displaying a binding pattern indistinguishable from the parental construct (Fig. 2C and D). Deletion of the CBD on the other hand, leaving only the two SH3b domains fused to GFP, radically altered the cell surface localization of the protein. Without the CBD, the GFP–SH3b–SH3b protein bound evenly across the cell envelope (Fig. 2E).

To determine whether the binding pattern obtained with the choline-binding domain of CbpD (CBD/D) is typical for proteins carrying this type of domain, we fused GFP to the choline-binding domain of CbpF (CBD/F), a protein reported to be a regulator of autolysis (Molina *et al.*, 2009). Our results show that the GFP–CBD/F construct exhibited an even distribution on the cell surface, illustrating that septum localization is not a general property of choline-binding proteins (Fig. 2F). The GFP–CBD/D construct contains a linker (N-QLEGVTSSQNYQNQSGNISSYGS-NNSSTV-C) between the GFP and the CBD/D. To test whether this linker could be involved in division zone

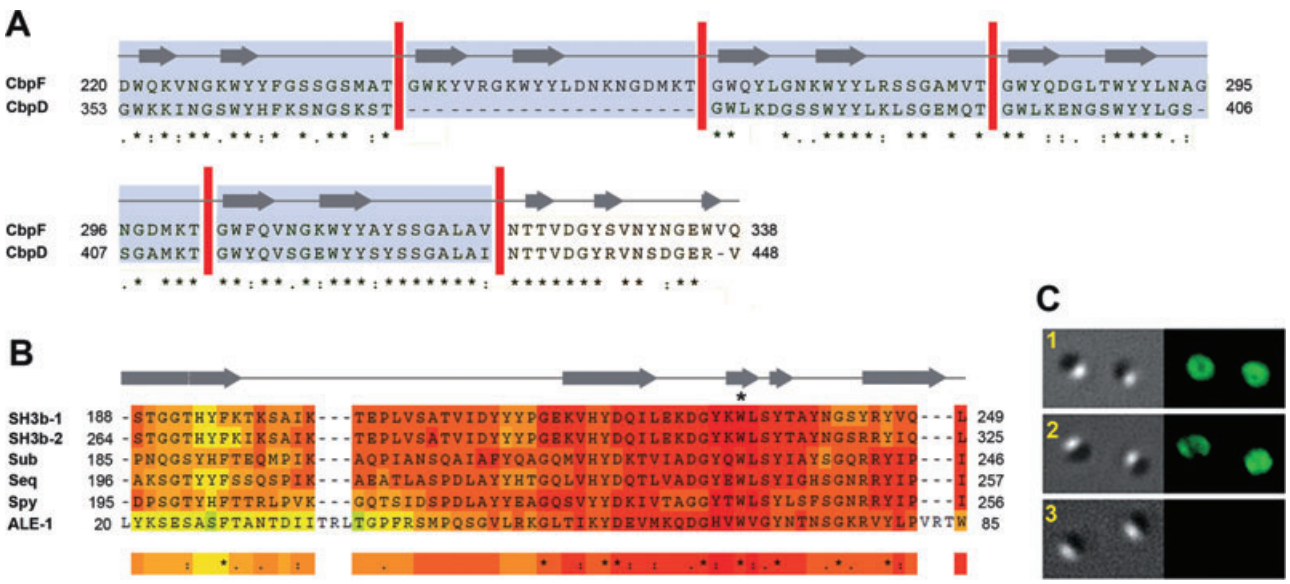

Fig. 3. Sequence analyses and binding studies of CBDs and SH3b domains.
A. Alignment of the CBDs (choline-binding repeats are shown in a shaded background and are separated by red bars) from CbpD and CbpF. The arrows above the alignment corresponds to β-strands in CbpF.
B. Alignment of the two SH3b domains from *Streptococcus pneumoniae* CbpD with SH3b domains from *Streptococcus pyogenes* CbpD, *Streptococcus uberis* CbpD, *Streptococcus suis* CbpD and *Staphylococcus aureus* ALE-1. The conserved tryptophan residue(s) chosen for site-directed mutagenesis is indicated by an asterisk. Colours indicate alignment score; from good (red) to poor (blue).
C. Binding of the GFP–SH3b–SH3b–CBD (1), GFP–SH3b–SH3b (2) and GFP–CBD (3) constructs to murein sacculi lacking teichoic acid. The sacculi were prepared from *S. pneumoniae* strain RH14.

targeting, it was inserted between GFP and CBD/F. In addition, another construct was made where the polar region (N-NYQNQSGNISSYGSNNSSTV-C) was removed from the GFP–CBD/D fusion protein. Neither of these changes affected the binding pattern of mutant proteins compared with their respective parental constructs (results not shown). In sum, these findings imply that CBD/D and CBD/F confer different binding specificities to the GFP fusion partner. Aligning the two CBDs using 3D-coffee (O'Sullivan *et al.*, 2004) that takes structural information into account [the structure of CbpF has been solved recently (Molina *et al.*, 2009)] reveals a high degree of conservation. The main difference is that CBD/D consists of four repeat units, whereas CBD/F has five (Fig. 3A).

The SH3b domains of CbpD bind peptidoglycan

SH3b domains are found in both Gram-positive and Gram-negative bacteria (Cabanes *et al.*, 2002). As mentioned above, the best-studied SH3b domains, with respect to their binding properties, are the targeting domains of the staphylococcal murein hydrolases lysostaphin and ALE-1 (Baba and Schneewind, 1996; Lu *et al.*, 2006). In these cases, the targeting domains recognize the pentaglycine interpeptide bridge characteristic of staphylococcal peptidoglycan. The pentaglycine bridge, however, is not recognized by SH3b itself, but by a separate binding motif consisting of nine amino acids situated at the N-terminal end of the SH3b domain (Lu *et al.*, 2006). A corresponding binding motif has not been found to be associated with SH3b-containing murein hydrolases from other bacterial species. The SH3b core domain is believed to bind peptidoglycan, but the specific portion of peptidoglycan recognized by SH3b has yet to be determined.

Having found that CbpD targets the cell envelope of *S. pneumoniae*, we decided to investigate whether the two SH3b domains are involved in peptidoglycan binding. We prepared cell wall sacculi from pneumococcal cells, and treated them with hydrofluoric acid to remove the teichoic acid component. The resulting sacculi, which consisted of pure peptidoglycan, bound the GFP–SH3b–SH3b–CBD fusion protein with an even distribution across the sacculi's surfaces (Fig. 3C). The GFP–SH3b–SH3b construct bound the sacculi in the same manner, whereas the GFP–CBD/D fusion protein was unable to bind. This finding demonstrates that the SH3b domains of CbpD specifically recognize the peptidoglycan component of the cell wall. It also shows that following hydrolysis of teichoic acid with hydrofluoric acid, the choline-binding domain is no longer able to mediate GFP-binding to pneumococcal sacculi.

Both the CBD and SH3b domains are required for efficient killing of non-competent cells during fratricide

After mapping the binding patterns of the fluorescent constructs described above, we wanted to investigate how

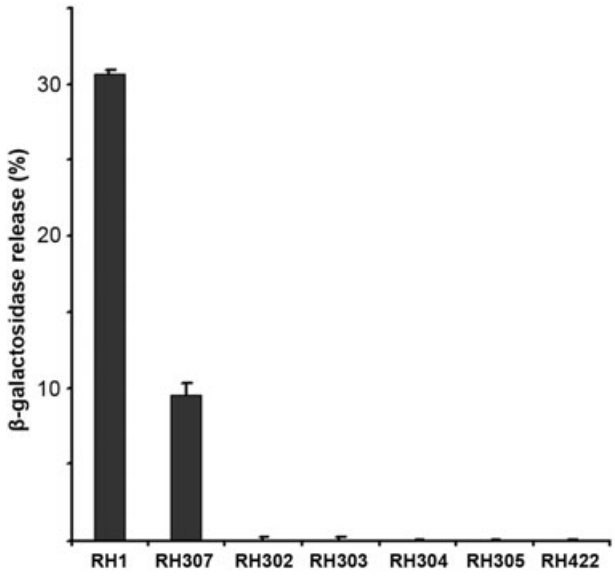

Fig. 4. Effect of specific mutations and domain deletions/alterations in CbpD on its ability to activate lysis of target cells. Lysis of target cells by attackers during co-cultivation experiments was determined by measuring the amount of intracellular β-galactosidase released to the growth medium relative to the total amounts of β-galactosidase present in the culture (target cells + medium). In all co-cultivation experiments RH3 (Δ*comE*, *hirL::lacZ*) was used as the target strain. The following strains were used as attackers: RH1 (produces wild-type CbpD), RH307 (produces CbpD chimera containing CBD from CbpF instead of its own CBD), RH302 (produces CbpD with deleted CBD), RH303 (produces CbpD lacking both SH3b domains), RH304 (produces CbpD with W310→A mutation in the C-terminal SH3b domain), RH305 (produces CbpD with W234→A and W310→A mutations in SH3b domains), RH422 (mutant with a deleted *cbpD* gene).

the corresponding alterations in the cell wall targeting domain of CbpD impacted on fratricide. During fratricide, CbpD produced by competent attacker cells triggers a chain of events that leads to lysis of non-competent target cells. All attacker strains used in this study were engineered to produce a CbpD variant with a functional CHAP domain, but carried the following mutations in other parts of the protein: deletion of CBD (RH302), deletion of both SH3b domains (RH303), W→A substitution in the C-terminal (RH304) or both (RH305) SH3b domains (see Fig. 3) or replacement of CBD/D with CBD/F from CbpF (RH307). These strains were compared with the wild-type attacker (RH1) in their ability to lyse non-competent target cells (RH3) upon competence induction (Fig. 4). RH3 cells constitutively express a β-galactosidase reporter protein that accumulates in the cytoplasm. Consequently, lysis of target cells by attackers during co-cultivation experiments can be monitored by measuring the amount of β-galactosidase released to the growth medium relative to the total amounts of β-galactosidase present in the culture (cells + medium) (Steinmoen *et al.*, 2002). Briefly, attacker strains and the target strain (RH3) were grown in C-medium to OD_{550} = 0.3. The attacker and target cultures were then mixed 1:1 concomitant with competence induction, and transferred to a 30°C water bath. After 30 min, β-galactosidase activity was measured in cell-free growth medium and total cell extracts. Based on these measurements the fraction of lysed target cells could be calculated.

Deletion of the two SH3b domains from CbpD completely abolished lysis of target cells during co-cultivation with competent attacker cells expressing this construct. The same result was obtained when the CBD/D domain was removed from the CbpD protein. Surprisingly, substituting a conserved tryptophan in only one of the two SH3b domains with an alanine (W_{310}→A) was enough to render the CbpD protein completely non-functional. Replacing the choline-binding domain of CbpD (CBD/D) with that of CbpF (CBD/F), on the other hand, resulted in a ~70% reduction in the lysis of target cells (Fig. 4). These results demonstrate that the dual binding of CbpD to teichoic acid and peptidoglycan via its choline-binding and SH3b domains, respectively, is essential for lysis of susceptible cells. The reduced lysis obtained upon substituting CBD/F for CBD/D indicates that CbpD functions more efficiently when it is directed to the septal region than when it binds to other parts of the pneumococcal cell wall.

CbpD causes ruptures in the division zone

Knowing that CbpD is a murein hydrolase, and that it localizes to the division zone, we used TEM to investigate whether CbpD mainly attacks this area of the cell wall. We took advantage of the fact that a subfraction (~20%) of cells lacking the immunity protein ComM lyse following competence induction (Håvarstein *et al.*, 2006). To avoid confusing the activity of CbpD with that of the autolysins LytA and LytC, both of which are activated by CbpD, we used a triple mutant (RH13) deficient in ComM, LytA and LytC for this experiment. The RH222 strain, containing an additional deletion of the *cbpD* gene, was used as a negative control. The strains were grown to OD_{550} = 0.3 and induced to competence. At time zero and 18 min after competence induction, 1 ml of samples of the cultures were withdrawn, mixed with 400 µl of ice-cold fixative and incubated on ice. EDTA has been shown to specifically enhance the effect of CbpD in the absence of LytA and LytC (Eldholm *et al.*, 2009). We therefore added 0.5 mM of this chelator to one parallel at the time of competence induction. Fixed and resin-embedded bacteria were thin-sectioned using ultramicrotomy, stained with uranyl acetate, and visualized using TEM. At time zero, there was no observable difference between the samples. Eighteen minutes after induction lysed cells could readily be seen in thin sections made from the RH13 cells, although the majority of the cells looked healthy (Fig. 5B). No lysed

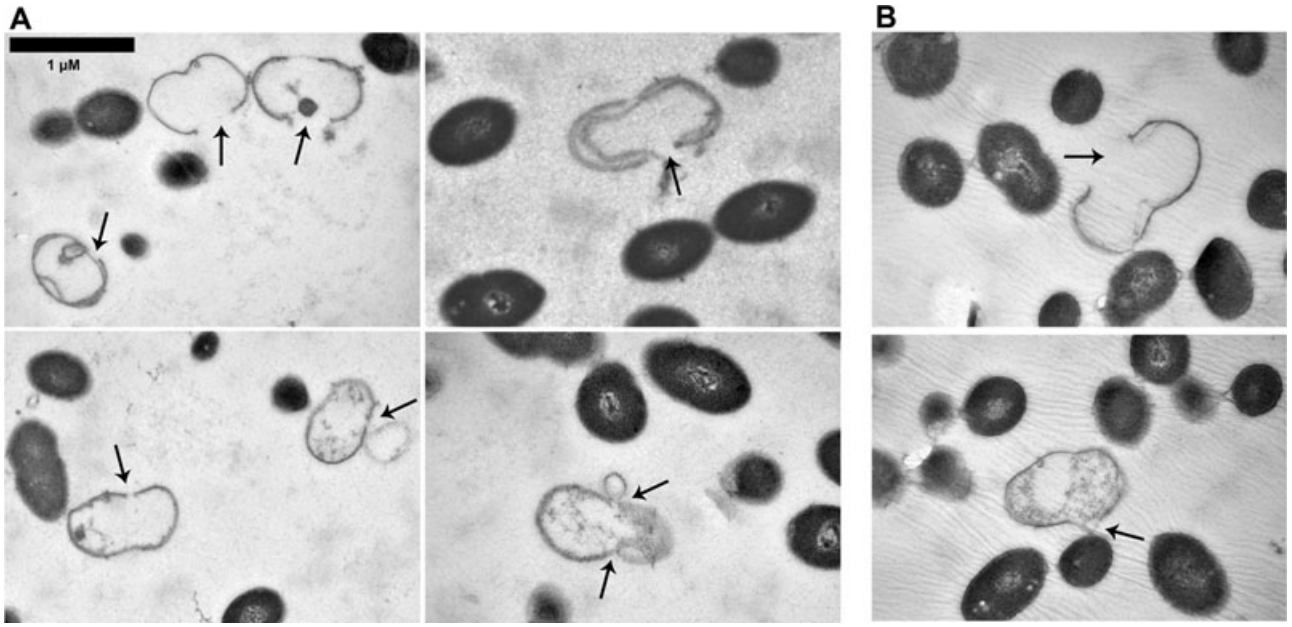

Fig. 5. Transmission electron micrographs of pneumococci 18 min after CSP induction. A Δ*lytA* Δ*lytC* double mutant (RH13) was used to specifically detect muralytic activity caused by CbpD. Lysis was most prominent in the presence of 0.5 mM EDTA (A), but lysed cells were also observed in the absence of EDTA (B). No lysed cells were found with the Δ*cbpD* Δ*lytA* Δ*lytC* triple mutant regardless of EDTA treatment (results not shown). Arrows indicate locations of cell rupture.

cells were seen in samples from CbpD-deficient RH222 cells (data not shown). In the presence of EDTA, lysis was more extensive in thin sections containing RH13 cells (Fig. 5A), whereas RH222 cells remained intact and seemingly healthy (data not shown). Intriguingly, in ruptured cells where the division zones are clearly visible, the cell wall was always split open in the septal region (Fig. 5). The fact that these ruptures only occur in the strain expressing CbpD demonstrates that this murein hydrolase is responsible for the observed cell wall damage. Together, our TEM data and results from the surface localization study outlined above strongly indicate that CbpD is a competence-specific murein hydrolase that predominantly attack the septal region of target cells.

Discussion

In the present work we have shown that the muralytic activity of CbpD depends on both its cell wall targeting domains. Furthermore, to cause efficient lysis CbpD must be directed towards the division zone of target cells, a function that is mediated by the enzyme's choline-binding domain.

Choline-decorated teichoic acid is found in *S. pneumoniae* and in a few closely related species; namely *Streptococcus pseudopneumoniae*, *S. mitis*, *S. oralis* and some strains of *Streptococcus infantis* (Kilian *et al.*, 2008). The implication of our findings is that the fractricide mechanism will be effective only when competent pneumococci encounter other strains or species containing choline-decorated teichoic acid in their cell walls. This is consistent with our previously published results demonstrating that *S. pneumoniae* can lyse members of the species *S. mitis* and *S. oralis*, but not *S. gordonii* (Johnsborg *et al.*, 2008). A consequence of the fratricide mechanism's limited target range is that it provides a means for competent cells to acquire homologous DNA. Interestingly, several streptococcal species lacking choline in their cell walls encode homologues of CbpD (Claverys *et al.*, 2007). However, in these cases the choline-binding domain has been exchanged with a completely unrelated type of domain with unknown properties. It is likely that this domain and CBD have equivalent functions, even though their binding specificities cannot be the same.

The SH3b domains of lysostaphin and its close homologue ALE-1 have both been shown to bind peptidoglycan from *S. aureus*. In the case of ALE-1, it was found that a nine-amino-acid motif adjacent to the classic SH3b domain recognizes the pentaglycine cross-bridge, explaining ALE-1's specificity for staphylococcal peptidoglycan. However, in the absence of this motif the SH3b domain of ALE-1 still retained some ability to bind purified peptidoglycan from *Lactobacillus plantarum*, a species that lacks interpeptide bridges between its stem peptides (Lu *et al.*, 2006). Interestingly, we found that our GFP–SH3b–SH3b construct binds to *L. plantarum* cells (result not shown). As the stem peptides of *L. plantarum* (L-Ala-D-iGlu-*meso*DAP-D-Ala-D-lactate) (Ferain *et al.*,

1996) are different from that of *S. pneumoniae* (L-Ala-D-iGln-L-Lys-D-Ala-D-Ala) (Garcia-Bustos *et al*., 1987), it is likely that the structure recognized by the SH3b domains of CbpD involves the conserved *N*-acetylglucosamine and/or *N*-acetylmuramic acid moieties. The sequence divergence between the SH3b domains of CbpD and the SH3b domain of ALE-1 is substantial (Fig. 3B), yet the fact that they all recognize peptidoglycan makes it tempting to speculate that this is a conserved role of bacterial SH3 domains. In addition to acting as targeting devices SH3b domains may also be crucial for substrate specificity by participating in the formation of the substrate-binding pocket together with the catalytic domain. This seems to be the case for AvPCP, a peptidoglycan cystein endopeptidase from *Anabaena variabilis* (Xu *et al*., 2009).

An important finding in the present study was that CbpD preferentially targets and ruptures the division zone. It is puzzling that CbpD should display such specificity considering that it is a 'weapon' produced by competent attacker cells to lyse and kill neighbouring target cells. Presumably, the fratricide mechanism would have been more efficient if CbpD was able to bind and hydrolyse any part of the cell wall instead of being directed towards a specific subsection of this megamolecule. One possible explanation is that the division zone represents the weakest part of the wall, and that CbpD as a result has evolved to target this region. In agreement with this, even distribution of the protein across the cell wall (by replacement of CBD/D with CBD/F) results in considerable reduction in lysis of target cells (Fig. 4). We speculate, however, that the restricted specificity of CbpD is an important part of the immunity mechanism that protects pneumococci against committing suicide during competence. It is likely that the immunity protein ComM, which in contrast to CbpD is encoded by an early competence gene, introduces a change in the peptidoglycan or teichoic acids of competent cells that blocks the activity of CbpD. Considering that ComM is expressed only a few minutes before CbpD, there might not be enough time to protect the whole cell wall. In addition, modification of the entire cell wall could be detrimental to the competent cell. If ComM only guards the cell division zone, however, protection can be achieved more quickly, and only a small part of the cell envelope will be transiently affected.

Very recently, Schlag *et al*. (2010) reported that WTA influences the cell surface localization of the staphylococcal Atl protein. This bifunctional autolysin is targeted to the cell-division zone via repeat domains that specifically recognizes and binds peptidoglycan. Interestingly, Schlag and co-workers' results suggest that the presence of WTA precludes or impairs binding of Atl to the peptidoglycan portion of the cell wall, and that Atl is able to bind to the septal region because this region does not contain WTA. Our results showed that the GFP–SH3b–SH3b–CBD construct targeted the septal region of sacculi even when they had been boiled in 4% SDS to remove LTA (data not shown), strongly indicating that WTA must be present in the septal region of pneumococcal cells. It follows from this that different mechanisms must be behind the observed septal positioning of CbpD and Atl. However, both mechanisms might depend on an uneven distribution of WTA and/or LTA across the bacterial cell surface.

Our results clearly show that it is the CBD and not the SH3b domains that targets CbpD to the septal region. To our knowledge, this is the first time that it has been demonstrated that a CBD alone is sufficient to target an entire/full-length protein to a specific location on the bacterial cell wall. Curiously, the targeting specificity displayed by CBD from CbpD is not common to all choline-binding proteins as the construct consisting of GFP fused to CBD from CbpF did not target the division zone, but displayed an approximately even distribution across the cell surface. This difference in location between the GFP–CBD/D and GFP–CBD/F constructs must be due to either subtle amino acid sequence differences or the number of choline-binding repeats. Interestingly, CbpD shows the lowest number of repeats among the members of the choline-binding family. Choline binding sites are formed at the interface of two consecutive repeats, where three aromatic residues non-covalently bind the choline moieties of teichoic acids. Considering the previously solved three-dimensional structure of CbpF (Molina *et al*., 2009) and the high sequence homology between CBDs of both proteins, it can be estimated that CBD/D could bind up to four choline moieties versus five for the CBD/F (Fig. S1), resulting in a lower choline affinity for CbpD than for CbpF. This dissimilarity together with subtle amino acid variations and/or modifications in the teichoic acid composition at the division zone could increase the choline affinity of CbpD at these specific loci. Alternatively, the higher choline-binding capability observed for CbpF could result in a less stringent binding requirement, allowing the protein to locate all across the cell surface.

Moreover, our experiments prove that the simultaneous presence of three separate cell wall targeting domains (the two SH3b domains plus the CBD) is required for CbpD activity. This contrasts with most pneumococcal choline-binding proteins, which only need a single targeting domain (a CBD) linked to the catalytic module to be fully active. As illustrated by the RH304 mutant strain, even a single-amino-acid substitution at one of the SH3b targeting domains completely abolishes the hydrolytic activity of CbpD. The unusual requirements observed for CbpD indicate that extremely precise recognition of the peptidoglycan is essential in order to obtain efficient and safe muralytic activity during fratricide.

In a previous study we found that lysis of target cells during fratricide only takes place in the presence of CbpD. However, fully efficient lysis required the presence of LytC

and LytA in addition to CbpD, strongly indicating that CbpD stimulates the muralytic activity of the two autolysins (Eldholm *et al*., 2009). In the present study we have obtained direct experimental evidence showing that CbpD and LytC together degrades the cell walls of pneumococci much more efficiently than CbpD alone (Fig. 1B). Very recently, Pérez-Dorado *et al*. (2010) proposed an explanation of this interesting phenomenon that is in full accordance with our findings. By determining for the first time the three-dimensional structure of LytC they were able to show that the modular configuration of LytC imposes limitations on its muralytic activity, and that prior cleavage of peptide stems by CbpD in theory could facilitate hydrolysis of non-cross-linked glycan strands by LytC. This means that during fratricide competent attacker cells lyse non-competent target cells by activating their autolysins. This amplification effect greatly enhances the impact of CbpD, and presumably allows the fratricide mechanism to function efficiently at a lower cost to the attacker cells.

In summary, we have reported here the function and localization of the multimodular murein hydrolase CbpD, which performs a highly regulated hydrolytic reaction on the cell wall peptidoglycan. Our experiments explain the co-ordinated role of the different modules of CbpD with respect to its lytic activity during pneumococcal fratricide. The particular composition of its choline-binding domain allows CbpD to target the division zone, while the presence of two in tandem SH3b domains attaches the protein to the peptidoglycan part of the cell wall. Most likely, the SH3b domains bind to the glycan strands and participate in the formation of the substrate-binding pocket together with the catalytic domain. Together our findings strongly indicate that the specific catalytic activity of CbpD set off a domino-like mechanism that activates LytC followed by LytA, resulting in rapid cell wall degradation and lysis of target cells.

Experimental procedures

Construction of S. pneumoniae *mutants*

Bacterial strains and plasmids used in this work are listed in Table 1, whereas the sequences of all primers used are given in Table S1. All *S. pneumoniae* transformations and experi-

Table 1. Strains and plasmids.

Strains/plasmids	Genotype/relevant feature	Reference/source
Strains		
RH1	*comA::ery, ebg::spc*, Ery^R, Spc^R	Johnsborg *et al*. (2008)
RH3	*comA::ery, ebg::spc, ΔcomE::kan, hirL*::pEVP3 (Cm^R), Ery^R, Spc^R, Kan^R, Cm^R	Johnsborg *et al*. (2008)
RH11	*comA::ery, ebg::spc, ΔcomE::kan, ΔlytA, ΔlytC::tc, hirL*::pEVP3 (Cm^R), Ery^R, Spc^R, Kan^R, Sm^R, Tc^R, Cm^R	Eldholm *et al*. (2009)
RH13	*comA::ery, ebg::spc, ΔcomM::Janus, ΔlytA, ΔlytC::tc, hirL*::pEVP3 (Cm^R), Ery^R, Spc^R, Kan^R, Tc^R, Cm^R	Eldholm *et al*. (2009)
RH14	*comA::ery, ebg::spc, ΔlytA::kan*, Ery^R, Spc^R, Kan^R	Eldholm *et al*. (2009)
RH15	*comA::ery, ebg::spc, ΔlytC::tc*, Ery^R, Spc^R, Tc^R	Eldholm *et al*. (2009)
RH16	*comA::ery, ebg::spc, ΔlytA::kan, ΔlytC::tc*, Ery^R, Spc^R, Kan^R, Tc^R	Eldholm *et al*. (2009)
RH17	*comA::ery, ebg::spc, ΔcbpD::kan*, Ery^R, Spc^R, Kan^R	Johnsborg *et al*. (2008)
RH222	*comA::ery, ebg::spc, ΔcomM::Janus, ΔlytA, ΔlytC::tc, ΔcbpD, hirL*::pEVP3 (Cm^R), Ery^R, Spc^R, Kan^R, Spc^R, Kan^R, Cm^R	Eldholm *et al*. (2009)
RH422	*comA::ery, ebg::spc, ΔcbpD::Janus*, Ery^R, Spc^R, Kan^R	Eldholm *et al*. (2009)
RH302	RH422 but *cbpDΔcbd*, Ery^R, Spc^R, Sm^R	This study
RH303	RH422 but *cbpDΔsh3-1 and Δsh3-2*, Ery^R, Spc^R, Sm^R	This study
RH304	RH422 but *cbpDW310→A*, Ery^R, Spc^R, Sm^R	This study
RH305	RH422 but *cbpDW234→A, W310→A*, Ery^R, Spc^R, Sm^R	This study
RH307	RH422 but *cbpD w/cbpF-CBD*, Ery^R, Spc^R, Sm^R	This study
E. coli BL21(DE3)pLysS	F^-, *ompT*, $hsdS_B$ (r_B^- m_B^-), *gal, dcm* (DE3), pLysS (Cm^R), Cm^R	Invitrogen
L. plantarum WCFS1		Kleerebezem *et al*. (2003)
Plasmids		
pRSET/EmGFP	*gfp*, Amp^R	Invitrogen
pVEG1	pRSET derivate carrying a *gfp–cbpD* fusion excluding the CHAP domain, Amp^R	This study
pVEG2	pRSET derivate carrying *gfp* fused to the two SH3 domains of *cbpD*, Amp^R	This study
pVEG3	pRSET derivate carrying *gfp* fused to the CBD of *cbpD* (including the SH3–CBD linker), Amp^R	This study
pVEGx3	pRSET derivate carrying *gfp* fused to the CBD of *cbpD*, Amp^R	This study
pVEGx4	pRSET derivate carrying a *gfp–cbpDW310→A* fusion excluding the CHAP domain, Amp^R	This study
pVEGx5	pRSET derivate carrying a *gfp–cbpDW234→A*, *W310→A* fusion excluding the CHAP domain, Amp^R	This study
pVEGF	pRSET derivate carrying *gfp* fused to the CBD of *cbpF*, Amp^R	This study
pVEGxF	pRSET derivate carrying *gfp* fused to the CBD of *cbpF* via a polar linker derived from *cbpD*, Amp^R	This study

ments were carried out in C-medium (Lacks and Hotchkiss, 1960). Bacterial cultures were grown at 37°C and induced to competence using 250 ng ml^{-1} synthetic CSP-1 (Genosphere Biotechnologies). The cells were subsequently mixed with the appropriate DNA and incubated for 2 h before plating on Todd Hewitt agar (Difco). Selection of mutants was carried out using the appropriate antibiotics at the following concentrations: streptomycin (Sm) 200 μg ml^{-1}, kanamycin (Kan) 400 μg ml^{-1}, spectinomycin (Spc) 200 μg ml^{-1}, chloramphenicol (Cm) 3.5 μg ml^{-1}, tetracycline (Tc) 0.2 μg ml^{-1}, erythromycin (Ery) 2.5 μg ml^{-1}.

In order to construct a *S. pneumoniae* strain lacking the CBD of *cbpD*, the primers CbpD-1098 and SH3R-DStail were used to amplify a DNA fragment encompassing the *cbpD* CHAP-encoding domain together with ~1000 bp of the *cbpD* upstream region. Next, a DNA fragment comprising ~1000 bp of the *cbpD* downstream region was amplified using the primers CbpD-DSF and CbpDR. Finally, the two PCR products were fused in a PCR using primers CbpD-1098 and CbpDR. The resulting DNA product was transformed into RH422, resulting in RH302.

To construct a strain expressing a *cbpD* lacking the two SH3b domains, the primers CbpD-1098 and CbpDCHAPR were used to amplify a DNA fragment encompassing the *cbpD* CHAP-encoding domain together with ~1000 bp of the *cbpD* upstream region. Next, a DNA fragment comprising the CBD-encoding domain together with ~1000 bp of the *cbpD* downstream region was amplified using the primers CBD-CHAPoverlapF and CbpDR. Finally, the two PCR products were fused in a PCR using primers CbpD-1098 and CbpDR. The resulting DNA product was transformed into RH422, resulting in RH303.

cbpD variants carrying one or two point mutated SH3-encoding domains were constructed as follows: the primers CbpD-1098 and CbpDCHAPR were used to amplify a DNA fragment encompassing the *cbpD* CHAP-encoding domain together with ~1000 bp of the *cbpD* upstream region. Next, the remaining part of the *cbpD* was amplified with primers SH3F-CHAPtail and CbpD-StopR, using 50 ng of pVEGx4 (contains a fragment of *cbpD* encoding the SH3b domain mutation $W{\rightarrow}A_{310}$) or pVEGx5 (contains a fragment of *cbpD* encoding the SH3b domain mutations $W{\rightarrow}A_{234} + W{\rightarrow}A_{310}$) as template respectively. The two resulting PCR products were separately fused to the CHAP encoding DNA fragment described above using the primers CbpD-1098 and CbpD-StopR. Finally, a ~1000 bp DNA fragment comprising the region downstream of *cbpD* was amplified using the primers CbpDFstop and CbpDR, and fused to the two DNA products (carrying full-length *cbpD* with point mutations in one or both SH3b domains) using the primers CbpD-1098 and CbpDR. The two PCR products, carrying a *cbpD* gene with one ($W{\rightarrow}A_{310}$) or two ($W{\rightarrow}A_{234} + W{\rightarrow}A_{310}$) mutated SH3b-encoding domains were transformed into RH422, resulting in RH304 and RH305 respectively.

To construct RH307, the CBD-encoding part of *cbpD* was switched with that from *cbpF*. First, the primers CbpD-1098 and CbpDlinkerR were used to amplify a DNA fragment comprising the parts of *cbpD* encoding the two SH3b domains, the CHAP domain, and ~1000 bp of the *cbpD* upstream region. Next, the CBD-encoding domain of *cbpF* was amplified with the primers CbpFCBDF and CbpFstopR, and subsequently fused to the fragment described above using the primers CbpD-1098 and CbpFstopR. Finally, a ~1000 bp fragment comprising the *cbpD* downstream region was amplified with the primers CbpDDSCbpFlink and CbpDR, and fused to the CHAP–SH3b–CBD-encoding fragment using the primers CbpD-1098 and CbpDR. The resulting fragments was transformed into RH422 resulting in RH307.

Construction of plasmids and expression of recombinant proteins

The gene encoding EmGFP was amplified from pRSET/EmGFP (Invitrogen) with the primers GfpFNheI and GfpR. *cbpD* excluding the CHAP-encoding domain was amplified with the primers SH3F and CbpDRXhoI. The two fragments were subsequently fused with the primers GfpFNheI and CbpDRXhoI. The resulting PCR construct was digested with NheI and XhoI and ligated into the plasmid pRSET pre-cleaved with the same enzymes. The resulting plasmid pVEG1 encodes a protein carrying a His-tagged GFP–CbpD fusion in which the GFP replaces the CHAP domain.

Various domains were fused to the gene encoding GFP following the method described above. The portion of *cbpD* encoding the two SH3b domains was amplified with the primers SH3F and SH3RXhoI. This fragment was fused to *gfp* as described above and ligated into pRSET resulting in pVEG2. The *cbpD* CBD-encoding domain including the CBD–SH3b linker domain was amplified with the primers CBDF and CbpDRXhoI, fused to *gfp* and ligated into pRSET yielding pVEG3. Using 50 ng of pVEG3 as template, the CBD domain without the SH3b linker was amplified with primers LinkDelF and CbpDRXhoI whereas *gfp* followed by the nine amino acids (QLEGVTSSQ) was amplified with the primers GfpFNheI and LinkDelR. The two PCR fragments were fused together with primers GfpFNheI and CbpDRXhoI and ligated into pRSET as described above, yielding pVEGx3.

The CBD-encoding domain of *cbpF* was amplified with the primers CbpFCBDGF and CbpFCBDRXhoI, fused to *gfp* and ligated into pRSET resulting in pVEGF.

gfp and the polar SH3b linker in pVEG3 were amplified with primers GfpFNheI and CbpDlinkerR. The CBD-encoding part of *cbpF* was amplified with the primers CbpFCBDF and CbpFCBDRXhoI. The fragments were fused using the primer pair GfpFNheI + CbpFCBDRXhoI, and ligated into pRSET resulting in pVEGxF.

To introduce a point mutation ($W_{310}{\rightarrow}A$) in one SH3b domain (SH3b-2), 20 ng of pVEG1 was used as template in a QuickChange PCR reaction with primers SH3W310A-F and SH3W310A-R using the non-strand-displacing Pfu Turbo polymerase (Stratagene). The procedure was carried out as described by the manufacturer. Following thermal cycling, the amplification products were treated with dpnI for 1 h. Five microlitres of the reaction was used to transform One Shot TOP10 Chemically Competent *E. coli* cells (Invitrogen). PCR screening and sequencing of the resulting clones identified a clone carrying the desired plasmid, designated pVEGx4. Following the same procedure, 20 ng of pVEGx4 was used as template in a QuickChange PCR reaction with primers SH3W234AR and SH3W234AF, resulting in the plasmid, pVEGx5, which contains a W→A substitution in the conserved tryptophan of both SH3 domains.

All plasmids were transformed into BL21(DE3)pLysS *E. coli* cells (Invitrogen) following the standard protocol. Expression of proteins was carried out at 30°C for 2 h with shaking. The cells were then lysed by repeated freezing and thawing in liquid nitrogen and a 42°C water bath. Recombinant proteins were purified with the aid of Protino Ni-TED columns (Macherey-Nagel).

Zymogram analysis of murein hydrolase activity

Zymograms were carried out as described by Leclerc and Asselin (1989) with some minor modifications. In brief, 50 μg of total protein (estimated by Coomassie blue staining) from different *S. pneumoniae* strains was separated by SDS-PAGE as described by Laemmli (1970) using a 4% stacking gel and a 10% resolving gel. Prior to polymerization, the resolving gel solution was mixed with heat-treated (95°C for 10 min) cells from a 300 ml culture $OD_{550} = 0.2$ of strain RH16 (ΔlytA, ΔLytC) (Eldholm *et al*., 2009). Following electrophoresis at 2.5 V cm^{-2}, the gels were washed in de-ionized water for 2 × 30 min before adding the refolding buffer (50 mM NaCl, 20 mM $MgCl_2$, 0.5% Triton X-100 and 20 mM Tris-HCl, pH 7.4). The gels were incubated in refolding buffer until the lytic zones could be observed in the turbid gel.

Fluorescence microscopy

Bacterial cells were grown to $OD_{550} = 0.4$, placed on ice and paraformaldehyde and glutaraldehyde added to a final concentration of 2.5% and 0.006% respectively. After 1 h, the cells were washed in PBS (pH 7.4) and fixed on slides (Thermo Scientific)

Pneumococcal cell wall sacculi were prepared as described by Reusch (1982) with some modifications. Briefly, 50 ml of bacteria at $OD_{550} = 0.35$ were pelleted and dissolved in 3.3 ml of extraction fluid containing 1% SDS + 0.5% β-mercaptoethanol (SDS-ME). The cells were incubated at 85°C for 15 min and dH_2O added to a final volume of 5 ml. The resulting gel was sonicated for 15 s and harvested at 17 680 *g* for 30 min. The pellet was dissolved in 3.3 ml of SDS-ME and extracted with hot SDS-ME five times. The extracted cells were washed five times with ddH_2O, once with 2 M NaCl, once with ddH_2O, once with 2 M NaCl and four times with ddH_2O. The cells were treated with trypsin (1.5 μg ml^{-1} in PBS) overnight and pelleted at 16 000 *g* and dissolved in 1 ml of 4% SDS. The cells were then incubated at 85°C for 15 min, washed thrice with dH_2O and dissolved in 100 μl of PBS. In order to remove covalently attached teichoic acids, 60 μl of the sacculi were pelleted and dissolved in 250 μl of 48% hydrofluoric acid. After 48 h of incubation at 4°C, the sacculi were harvested by centrifugation at 16 000 *g* for 20 min, washed thrice with dH_2O and dissolved in 50 μl of PBS.

Slides with sacculi or fixed cells were incubated in room temperature for 8 min with ~15 μg ml^{-1} fluorescent fusion protein dissolved in PBS containing 0.05% Tween-20. When appropriate, 5 μg ml^{-1} DAPI was added to the protein solution. Following incubation, the slides were washed thrice for 1 min with in PBS containing 0.05% Tween-20.

Transmission electron microscopy

Pneumococci were grown at 37°C to $OD_{550} = 0.3$, induced to competence with CSP (250 ng ml^{-1}) and incubated at 30°C. In a parallel experiment, EDTA was added to a final concentration of 0.5 mM at the time of competence induction. At 0 and 18 min post induction, 1 ml of the cultures were withdrawn, added to 400 μl of ice-cold fix (7.5% paraformaldehyde + 0.018% glutaraldehyde) and incubated on ice. After 1 h of incubation, the cells were washed with PBS buffer, embedded in 0.5% low melting agarose, and further fixed with 2.5% paraformaldehyde and 0.006% glutaraldehyde overnight at 4°C. The cells were subsequently washed 3× with cacodylate buffer (0.1 M, pH 6.8), and post-fixed with 1% osmium in cacodylatbuffer for 1 h at 4°C. Subsequently, the cells were washed several times with cacodylate buffer and dehydrated with a graded series of ethanol (50%, 70%, 90%, 96% and 4× 100%), using 10 min incubations for each step. Finally, the cells were embedded in LRWhite resin. Ultrathin sections were cut with a diamond knife mounted on an ultramicrotome (LEICA EM UC 6) and sections were picked up with formvar- and carbon-coated slot copper grids. Counterstaining of the sections was performed with 4% aqueous uranyl acetate and 1% $KMNO_4$ for 10 min. The sections were examined with a FEI MORGAGNI 268 transmission electron microscope at an accelerating voltage of 80 kV, and photographs were recorded on VELETA camera.

Sequence alignments

Alignments were performed using 3D-coffee (O'Sullivan *et al*., 2004) as implemented in the phylogeny.fr package (Dereeper *et al*., 2008). The alignment of the CBD of *cbpD* and *cbpF* was curated by hand after aligning with 3D-coffe.

β-Galactosidase assay

β-Galactosidase assays to measure cell lysis was carried out as described previously (Steinmoen *et al*., 2002).

Acknowledgements

The authors would like to thank Hilde Kolstad at the IPM imaging laboratory for technical assistance with the TEM analysis. This work was supported by The Research Council of Norway.

References

Baba, T., and Schneewind, O. (1996) Target cell specificity of a bacteriocin molecule: a C-terminal signal directs lysostaphin to the cell wall of *Staphylococcus aureus*. *EMBO J* **15:** 4789–4797.

Bateman, A., and Rawlings, N.D. (2003) The CHAP domain: a large family of amidases including GSP amidase and peptidoglycan hydrolases. *Trends Biochem Sci* **28:** 234–237.

Cabanes, D., Dehoux, P., Dussurget, O., Frangeul, L., and Cossart, P. (2002) Surface proteins and the pathogenic potential of *Listeria monocytogenes*. *Trends Microbiol* **10:** 238–245.

Claverys, J.-P., and Håvarstein, L.S. (2007) Cannibalism and fratricide: mechanisms and raisons d'être. *Nat Rev Microbiol* **5:** 219–229.

Claverys, J.-P., Martin, B., and Håvarstein, L.S. (2007) Competence-induced fratricide in streptococci. *Mol Microbiol* **64:** 1423–1433.

Dereeper, A., Guignon, V., Blanc, G., Audic, S., Buffet, S., Chevenet, F., *et al*. (2008) Phylogeny.fr: robust phylogenetic analysis for the non-specialist. *Nucleic Acids Res* **36:** W465–W469.

Eldholm, V., Johnsborg, O., Haugen, K., Ohnstad, H.S., and Håvarstein, L.S. (2009) Fratricide in *Streptococcus pneumoniae*: contributions and role of the cell wall hydrolases CbpD, LytA and LytC. *Microbiology* **155:** 2223–2234.

Ferain, T., Hobbs, J.N., Richardson, J., Bernard, N., Garmyn, D., Hols, P., *et al*. (1996) Knockout of the two *ldh* genes has a major impact on peptidoglycan precursor synthesis in *Lactobacillus plantarum*. *J Bacteriol* **178:** 5431–5437.

García, P., González, M.P., García, E., García, J.L., and López, R. (1999) The molecular characterization of the first autolytic lysozyme of *Streptococcus pneumoniae* reveals evolutionary mobile domains. *Mol Microbiol* **33:** 128–138.

Garcia-Bustos, J.F., Chait, B.T., and Tomasz, A. (1987) Structure of the peptide network of pneumococcal peptidoglycan. *J Biol Chem* **262:** 15400–15405.

Guiral, S., Mitchell, T.J., Martin, B., and Claverys, J.-P. (2005) Competence-programmed predation of noncompetent cells in the human pathogen *Streptococcus pneumoniae*: genetic requirements. *Proc Natl Acad Sci USA* **102:** 8710–8715.

Hakenbeck, R., Madhour, A., Denapaite, D., and Brückner, R. (2009) Versatility of choline metabolism and choline-binding proteins in *Streptococcus pneumoniae* and commensal streptococci. *FEMS Microbiol Rev* **33:** 572–586.

Håvarstein, L.S., Coomaraswamy, G., and Morrison, D.A. (1995) An unmodified heptadecapeptide pheromone induces competence for genetic transformation in *Streptococcus pneumoniae*. *Proc Natl Acad Sci USA* **92:** 11140–11144.

Håvarstein, L.S., Gaustad, P., Nes, I.F., and Morrison, D.A. (1996) Identification of the streptococcal competence-pheromone receptor. *Mol Microbiol* **21:** 863–869.

Håvarstein, L.S., Martin, B., Johnsborg, O., Granadel, C., and Claverys, J.-P. (2006) New insights into the pneumococcal fratricide: relationship to clumping and identification of a novel immunity factor. *Mol Microbiol* **59:** 1297–1307.

Johnsborg, O., and Håvarstein, L.S. (2009) Regulation of natural genetic transformation and acquisition of transforming DNA in *Streptococcus pneumoniae*. *FEMS Microbiol Rev* **33:** 627–642.

Johnsborg, O., Eldholm, V., Bjørnstad, M.L., and Håvarstein, L.S. (2008) A predatory mechanism dramatically increases the efficiency of lateral gene transfer in *Streptococcus pneumoniae* and related commensal species. *Mol Microbiol* **69:** 245–253.

Kausmally, L., Johnsborg, O., Lunde, M., Knutsen, E., and Håvarstein, L.S. (2005) Choline-binding protein D (CbpD) in *Streptococcus pneumoniae* is essential for competence-induced cell lysis. *J Bacteriol* **187:** 4338–4345.

Kilian, M., Poulsen, K., Blomqvist, T., Håvarstein, L.S., Bek-Thomsen, M., Tettelin, H., and Sørensen, U.B.S. (2008) Evolution of *Streptococcus pneumoniae* and its close commensal relatives. *PLoS ONE* **3:** e2683.

Kleerebezem, M., Boekhorst, J., van Kranenburg, R., Molenaar, D., Kuipers, O.P., Leer, R., *et al*. (2003) Complete genome sequence of *Lactobacillus plantarum* WCFS1. *Proc Natl Acad Sci USA* **100:** 1990–1995.

Lacks, S., and Hotchkiss, R.D. (1960) A study of the genetic material determining an enzyme in pneumococcus. *Biochim Biophys Acta* **39:** 508–518.

Laemmli, U.K. (1970) Cleavage of structural proteins during the assembly of the head of bacteriophage T4. *Nature* **227:** 680–685.

Layec, S., Gérard, J., Legué, V., Chapot-Chartier, M.-P., Courtin, P., Borges, F., *et al*. (2009) The CHAP domain of Cse functions as an endopeptidase that acts at mature septa to promote *Streptococcus thermophilus* cell separation. *Mol Microbiol* **71:** 1205–1217.

Leclerc, D., and Asselin, A. (1989) Detection of bacterial cell wall hydrolases after denaturing polyacrylamide gel electrophoresis. *Can J Microbiol* **35:** 749–753.

Lee, M.S., and Morrison, D.A. (1999) Identification of a new regulator in *Streptococcus pneumoniae* linking quorum sensing to competence for genetic transformation. *J Bacteriol* **181:** 5004–5016.

López, R., González, M.P., García, E., García, J.L., and García, P. (2000) Biological roles of two murein hydrolases of *Streptococcus pneumoniae* representing examples of module shuffling. *Res Microbiol* **151:** 437–443.

Lu, J.Z., Fujiwara, T., Komatsuzawa, H., Sugai, M., and Sakon, J. (2006) Cell wall-targeting domain of glycylglycine endopeptidase distinguishes among peptidoglycan cross-bridges. *J Biol Chem* **281:** 549–558.

Molina, R., González, A., Stelter, M., Pérez-Dorado, I., Kahn, R., Morales, M., *et al*. (2009) Crystal structure of CbpF, a bifunctional choline-binding protein and autolysis regulator from *Streptococcus pneumoniae*. *EMBO Rep* **10:** 246–251.

Mortier-Barrière, I., de Saizieu, A., Claverys, J.-P., and Martin, B. (1998) Competence-specific induction of *recA* is required for full recombination proficiency during transformation in *Streptococcus pneumoniae*. *Mol Microbiol* **27:** 159–170.

O'Sullivan, O., Suhre, K., Abergel, C., Higgins, D.G., and Notredame, C. (2004) 3DCoffee: combining protein sequences and structures within multiple sequence alignments. *J Mol Biol* **340:** 385–395.

Pérez-Dorado, I., González, A., Morales, M., Sanles, R., Striker, W., Vollmer, W., *et al*. (2010) Insights into pneumococcal fratricide from crystal structure of the modular killing factor LytC. *Nat Struct Mol Biol* (in press).

Pestova, E.V., Håvarstein, L.S., and Morrison, D.A. (1996) Regulation of competence for genetic transformation in *Streptococcus pneumoniae* by an auto-induced peptide pheromone and a two-component regulatory system. *Mol Microbiol* **21:** 853–862.

Reusch, V.M., Jr (1982) Isolation and analysis of sacculi from *Streptococcus sanguis*. *J Bacteriol* **151:** 1543–1552.

Rigden, D.J., Jedrzejas, M.J., and Galperin, M.Y. (2003) Amidase domains from bacterial and phage autolysins define a family of γ-D,L-glutamate-specific amidohydrolases. *Trends Biochem Sci* **28:** 230–234.

Schlag, M., Biswas, R., Krismer, B., Kohler, T., Zoll, S., Yu, W., *et al*. (2010) Role of staphylococcal wall teichoic acid in targeting the major autolysin Atl. *Mol Microbiol* **75:** 864–873.

Steinmoen, H., Knutsen, E., and Håvarstein, L.S. (2002) Induction of natural competence in *Streptococcus pneumoniae* triggers lysis and DNA release from a subfraction of the cell population. *Proc Natl Acad Sci USA* **99:** 7681–7686.

Varea, J., Saiz, J.L., López-Zumel, C., Monterroso, B., Medrano, F.J., Arrondo, J.L.R., *et al*. (2000) Do sequence repeats play an equivalent role in the choline-binding module of pneumococcal LytA amidase? *J Biol Chem* **275:** 26842–26855.

Ween, O., Gaustad, P., and Håvarstein, L.S. (1999) Identification of DNA binding sites for ComE, a key regulator of natural competence in *Streptococcus pneumoniae*. *Mol Microbiol* **33:** 817–827.

Whisstock, J.C., and Lesk, A.M. (1999) SH3 domains in prokaryotes. *Trends Biochem Sci* **24:** 132–133.

Wu, H., Reynolds, A.B., Kanner, S.B., Vines, R.R., and Parsons, J.T. (1991) Identification and characterization of a novel cytoskeleton-associated pp60src substrate. *Mol Cell Biol* **11:** 5113–5124.

Xu, Q., Sudek, S., McMullan, D., Miller, M.D., Geierstanger, B., Jones, D.H., *et al*. (2009) Structural basis of murein peptide specificity of a γ-D-Glutamyl-L-Diamino acid endopeptidase. *Structure* **17:** 303–313.

Supporting information

Additional supporting information may be found in the online version of this article.

Please note: Wiley-Blackwell are not responsible for the content or functionality of any supporting materials supplied by the authors. Any queries (other than missing material) should be directed to the corresponding author for the article.